Electronic supplementary information

Iron Oxide Nanorods as High–Performance Magnetic Resonance Imaging Contrast Agents

Jeotikanta Mohapatra,[1] Arijit Mitra,[2] Himanshu Tyagi,[2] D. Bahadur,[1, 3, *] M. Aslam[1, 2, *,╫]

[1] Centre for Research in Nanotechnology and Science (CRNTS), [2] Department of Physics,

[3] Department of Metallurgical Engineering and Materials Science, Indian Institute of Technology Bombay, Powai, Mumbai-400076, India

**To whom correspondence should be addressed. E-mail: m.aslam@iitb.ac.in (M. Aslam). Phone: +91 22 2576 7585, dhirenb@iitb.ac.in (D. Bahadur), +91-22-2576 7632*

╫Visiting scholar, Materials Science and Engineering Department, Northwestern Univeristy, Evanston, IL-60201

(A) Theoretical basis of proton transverse relaxivity

According to quantum-mechanical outer-sphere theory, the R_2 relaxivity of iron oxide nanoparticles in solution can be given by

$$R_2 = \left(\frac{256\pi^2\gamma^2}{405}\right) kM_S^2 d^2 / \mathrm{D}(1 + \mathrm{L}/\mathrm{d}) \text{ ....S1}$$

where γ is the proton gyromagnetic ratio, k, M_S, and d are the volume fraction, saturation magnetization and the effective diameter, respectively, D is the diffusivity of water molecules and L is the thickness of the impermeable surface coating. This theory predicts that the R_2 relaxivity of iron oxide nanoparticles increases with the M_S and the effective diameter d if the total amount of iron, k, is constant.

(B) Surface functionalization

Fig. S1: Illustration of the surface modification of Fe_3O_4 NRs by PEI. 100 mg of the as prepared Fe_3O_4 NRs were sonicated in 10 ml of toluene and after complete dispersion 2 ml of PEI solution with 10 ml of dimethylformamide (DMF) was added to this mixture. Under N_2 ambience, the mixture was then continuously stirred at 80 °C for 8 h. After the reaction, the final product was subjected to magnetic separation and was washed several times with ethanol to remove uncoordinated PEI molecules. The resultant PEI functionalized Fe_3O_4 NRs were dispersed easily in deionized water.

(C) Crystal structure and morphology

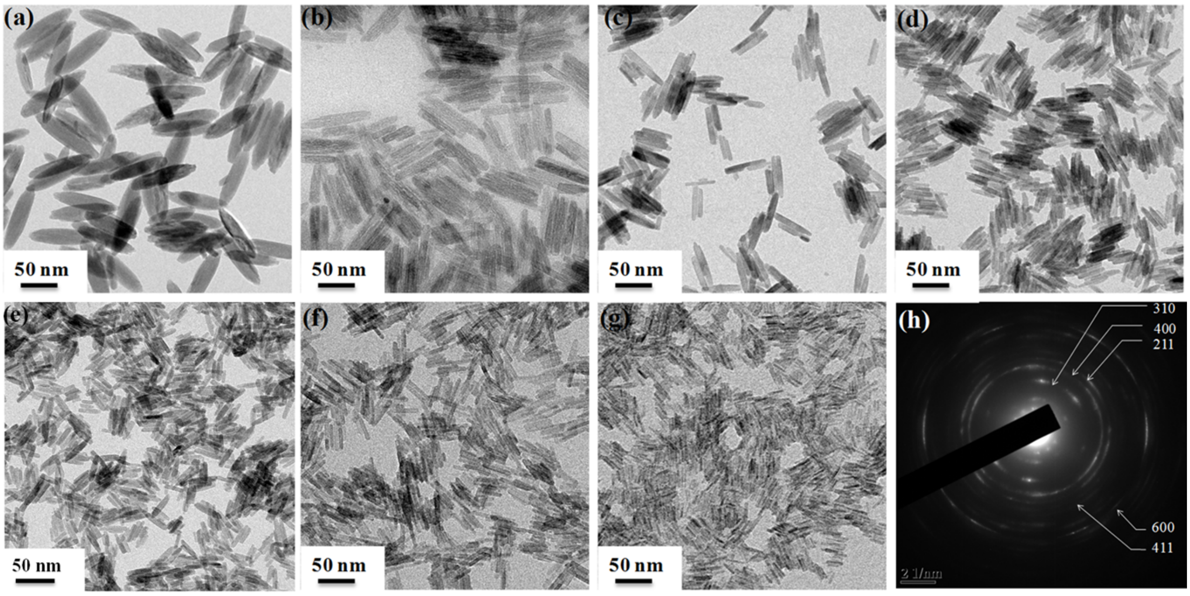

Fig. S2: TEM micrographs of FeOOH NRs of different length, produced by using: (a) 0.1 ml, (b) 0.2 ml, (c) 0.3 ml, (d) 0.5 ml, (e) 1 ml, (f) 1.5 ml and (g) 2 ml of PEI as a capping agent. The average lengths of NRs obtained are 25 ± 4 nm, 30 ± 5 nm, 40 ± 5 nm, 50 ± 5 nm, 70 ± 10 nm and 110 ± 15 nm for 2 ml, 1.5 ml, 1 ml, 0.5 ml, 0.2 ml and 0.1 ml of PEI, respectively. The effect of PEI amount on shape, length and diameter of FeOOH particles is summarized in Table S1. This control over nanords length and diameter with the PEI content is due to the adsorption of the protonized PEI on the lateral plane (200) of the rods. (h) The SAED pattern shows a set of rings identified as reflection from five crystal planes (310), (400), (211), (411) and (600) of FeOOH NRs.

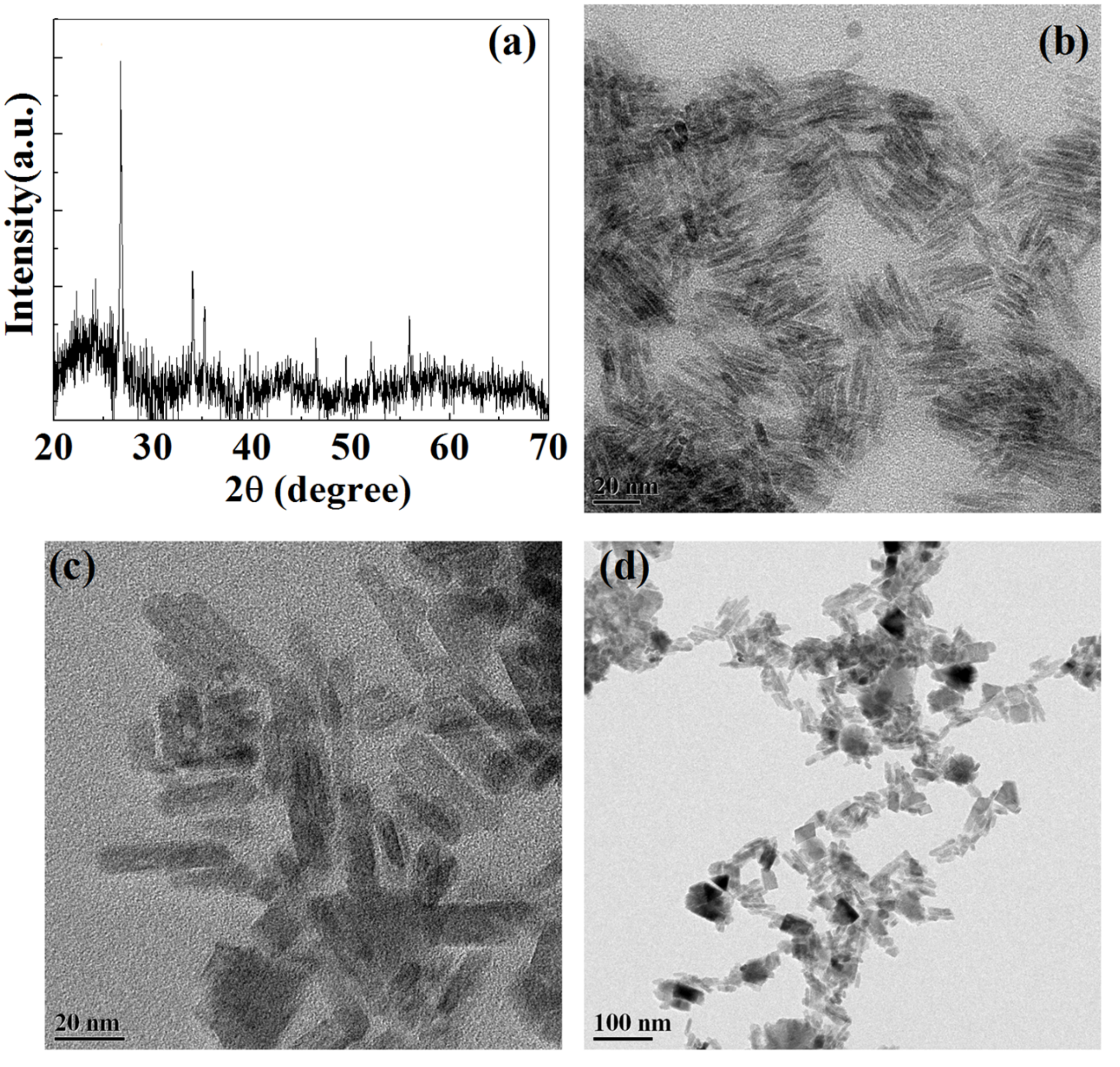

Fig. S3: (a) XRD pattern of FeOOH NRs produced by using 2 ml PEI as capping agent. The absence of diffraction peaks in FeOOH sample indicates the poor crystallinity of the prepared NRs. (b) The corresponding TEM image, the average length of NR obtained is 25 ± 4 nm. (c) and (d) the high and low magnification TEM images of Fe_3O_4 NRs obtained after reducing the 25 nm length FeOOH NRs to Fe_3O_4.

.

(D) Thermogravimetric analysis

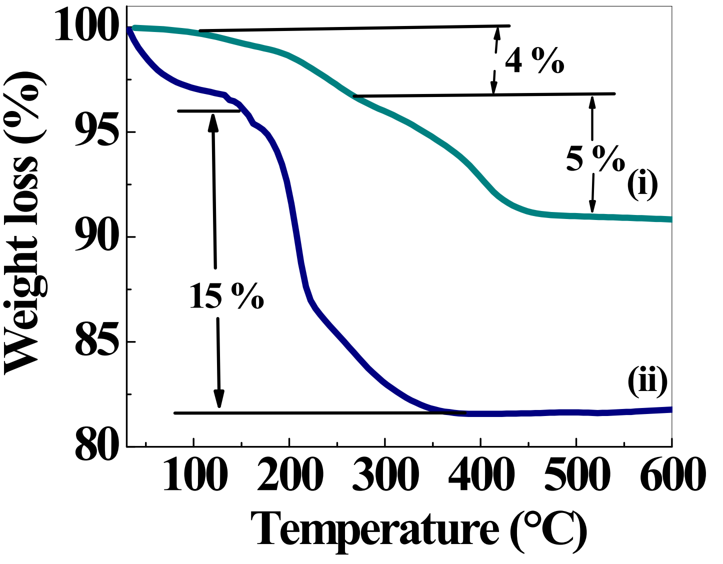

Fig. S4: Thermogravimetric plot of Fe_3O_4 NRs of length 70 nm; (i) as prepared (oleylamine coated NRs) and (ii) PEI functionalized. The PEI and oleylamine coated NRs shows weight loss of 15 % and 9 % over a temperature range of 150-450 °C respectively, attributed to decomposition of the organic molecules attached to the NRs surface. The increases of 6 % weight loss after surface modification of NRs with PEI confirm the presence of PEI on NRs surface.

(E) Colloidal stability

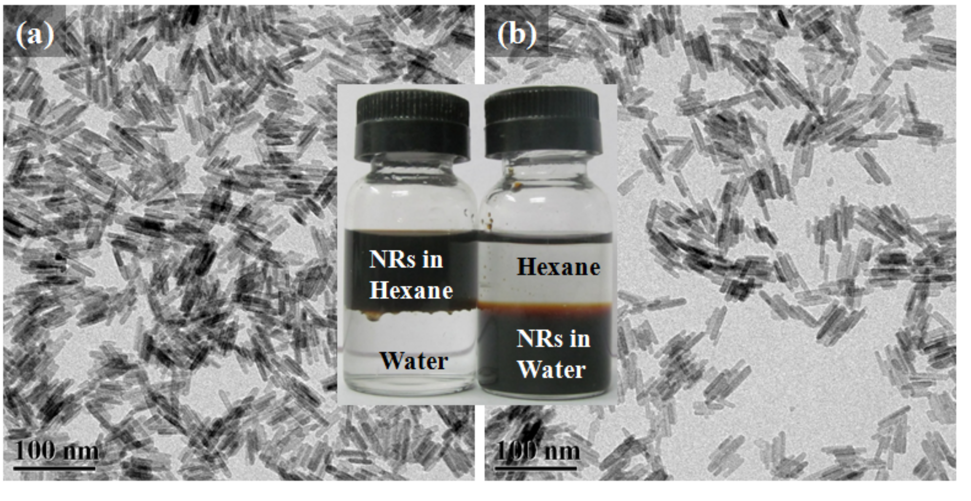

Fig. S5: TEM micrographs of Fe_3O_4 NRs of length 50 nm (a) as prepared (oleylamine coated NRs) and (b) PEI functionalized.

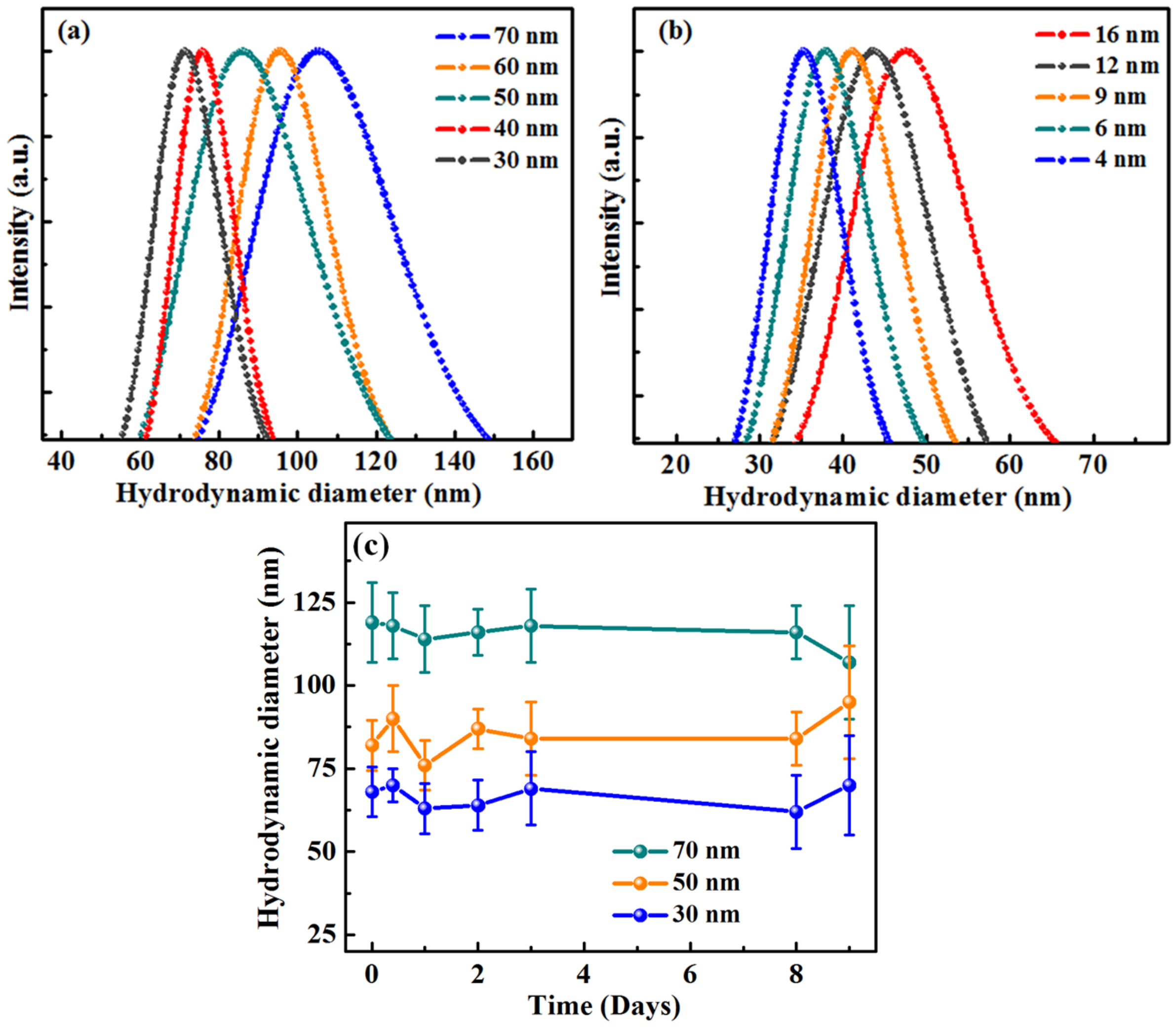

Fig. S6: Hydrodynamic diameter of different sized Fe_3O_4: (a) NRs and (b) SNPs encapsulated with PEI. (c) Time dependent studies show the average hydrodynamic size of PEI functionalized Fe_3O_4 NRs as a function of time.

(F) Cell viability study

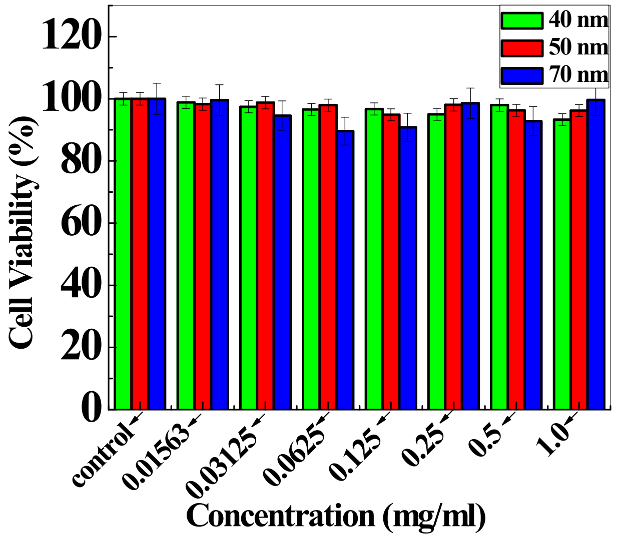

Fig. S7: Percentage viability of HeLa cells after 24 h incubation of stable aqueous suspension of PEI functionalized Fe_3O_4 NRs of different lengths. The results are shown as mean ± standard deviation (n = 3).

(G) Local magnetic field calculation

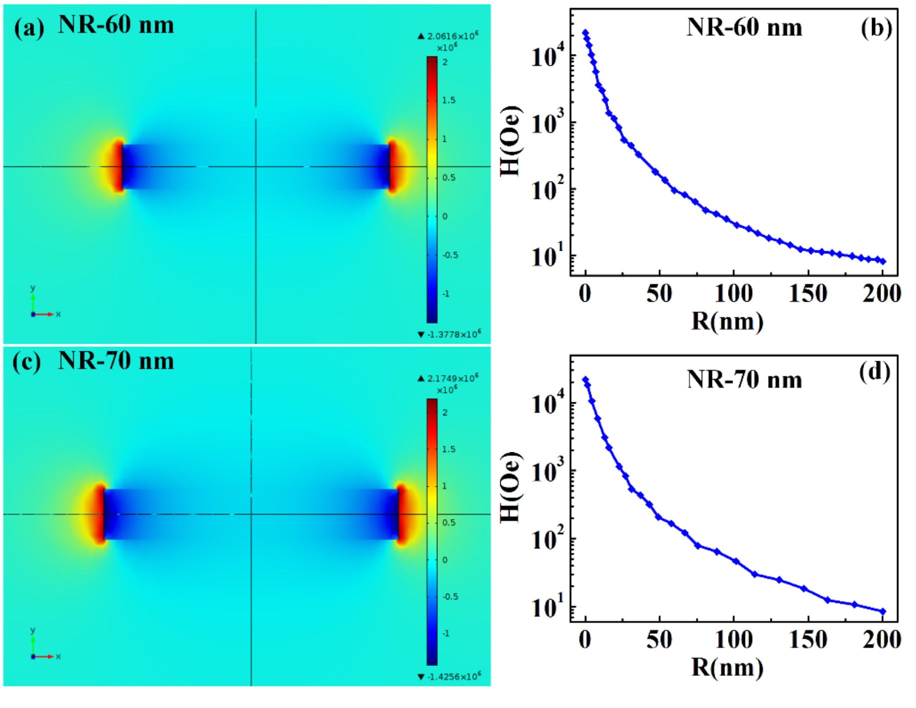

Fig. S8: The local magnetic field generated by Fe_3O_4 nanorods of length: (a) 60 nm and (c) 70 nm under an applied magnetic field of 3T. (b) and (d) show the variation of induced magnetic field with distance 'R' from the surface of nanorods (y-axis is in log scale).

Table S1: Effect of PEI content on shape, length and diameter of FeOOH nanostructures.

PEI content	Shape	Length (nm)	Diameter (nm)	Aspect ratio
2	rod	25	3	8.3
1.5	rod	30	4	7.5
1	rod	40	6	6.6
0.5	rod	50	8	6.25
0.3	rod	60	10	6
0.2	rod	70	12	5.8
0.1	spindle	110	24	4.5
0	spindle	150	35	4.2

Table S2: Hydrodynamic size, saturation magnetization, R_2 relaxivity of Fe_3O_4 NRs of different lengths.

Sample Code	Hydrodynamic size (nm)	M_S (emu/g)	R_2 Relaxivity (s^{-1} mM^{-1})
NR 30	71	50	312
NR 40	76	54	381
NR 50	86	58	427
NR 60	95	63	545
NR 70	105	66	608

Table S3: Hydrodynamic size, saturation magnetization, R_2 relaxivity of spherical shape Fe_3O_4 nanoparticles of different diameters.

Sample Code	Diameter (nm) (d ± 1 nm)	Hydrodynamic size (nm)	M_S (emu/g)	R_2 Relaxivity (s^{-1} mM^{-1})
SNP 4	4	35	56	141
SNP 6	6	38	63	185
SNP 8	8	41	70	218
SNP 12	12	44	78	249
SNP 16	16	48	83	297

Table S4: Effective diameter, material volume and surface area of different sized Fe_3O_4 NRs and their equivalent material volume spherical NPs.

Nanorods				**Spherical Nanoparticles**		**Surface area ratio of NR to NP** (A_{NR}/A_{NP})
Length (L ± 5 nm)	Diameter (d_{NR} ± 1 nm)	Volume 'V_{NR}' (nm^3)	Surface area 'A_{NR}' (nm^2)	Diameter (d_{NP} ± 1.2 nm nm)	Surface area 'A_{NP}' (nm^2)	
30	4	376	402	8.9	252	1.5
40	6	1130	810	12.9	524	1.5
50	8	2513	1357	16.8	893	1.5
60	10	4712	2042	20.8	1359	1.5
70	12	7916	2865	24.7	1920	1.5